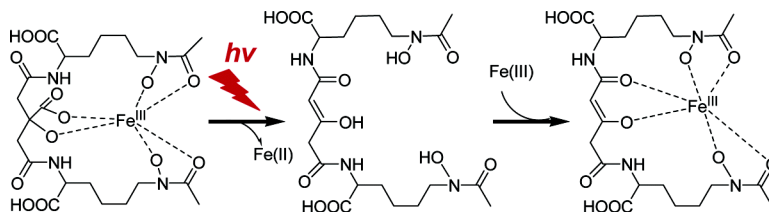


Photoreactivity of Iron(III)–Aerobactin: Photoproduct Structure and Iron(III) Coordination

Frithjof C. Kpper, Carl J. Carrano, Jens-Uwe Kuhn, and Alison Butler

Inorg. Chem., **2006**, 45 (15), 6028-6033 • DOI: 10.1021/ic0604967 • Publication Date (Web): 24 June 2006

Downloaded from <http://pubs.acs.org> on March 2, 2009



More About This Article

Additional resources and features associated with this article are available within the HTML version:

- Supporting Information
- Links to the 2 articles that cite this article, as of the time of this article download
- Access to high resolution figures
- Links to articles and content related to this article
- Copyright permission to reproduce figures and/or text from this article

[View the Full Text HTML](#)

Photoreactivity of Iron(III)–Aerobactin: Photoproduct Structure and Iron(III) Coordination

Frithjof C. Küpper,[†] Carl J. Carrano,[‡] Jens-Uwe Kuhn,[†] and Alison Butler^{*†}

Departments of Chemistry and Biochemistry, University of California, Santa Barbara, California 93106-9510, and San Diego State University, San Diego, California 92182-1030

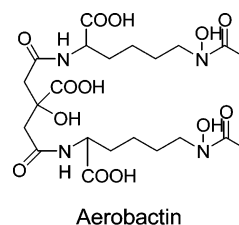
Received March 24, 2006

UV photolysis of the ferric aerobactin complex results in decarboxylation of the α -hydroxy carboxylic acid group of the central citrate moiety of aerobactin. The structure determination of the photooxidized ligand shows that decarboxylation occurs at the citrate moiety forming a 3-ketoglutarate moiety. Proton and carbon-13 NMR establish the presence of keto and enol tautomers of the apo-photoproduct, with the enol form prevailing in water. The photoproduct retains the ability to coordinate iron(III). The values of the ligand protonation constants, the pK_a of the Fe(III)–ligand complex, and the Fe(III) stability constant of the photoproduct of aerobactin are all close to those of aerobactin. CD spectroscopy suggests that the chirality of the ferric complexes of aerobactin and its photoproduct are similar. Like aerobactin, the photoproduct promotes iron acquisition by the source bacterium, *Vibrio sp.* DS40M5.

Introduction

Siderophores are low-molecular-weight compounds produced by many bacteria to facilitate the acquisition of iron.^{1,2} A striking feature of many siderophores produced by oceanic bacteria is the prevalence of α -hydroxy carboxylic acid functionalities,³ either in the form of the amino acid β -hydroxyaspartic acid^{4,5} or in the form of citric acid.^{6–8} The marine β -hydroxyaspartic acid-containing siderophores include the alterobactins A and B,⁴ as well as the amphiphilic aquachelin and marinobactin siderophores.⁵ The marine citric

acid-containing siderophores include aerobactin (see structure below),⁶ petrobactin,⁷ and the amphiphilic synechobactins,⁸ among others.



In addition to the discovery of aerobactin produced by marine bacteria, such as *Vibrio sp.* DS40M5 used in this report,⁶ aerobactin has long been known as the siderophore of the lung pathogen *Klebsiella pneumoniae*⁹ and has been isolated from a considerable diversity of other bacteria, including *Escherichia coli*¹⁰ and plant pathogens.¹¹

Ferric complexes of α -hydroxy carboxylic acid siderophores are photoreactive, as is well known for ferric citrate complexes.¹² Photoexcitation into the α -hydroxy-acid-to-Fe(III) charge-transfer band in the UV induces formation of

* To whom correspondence should be addressed. E-mail: Butler@chem.ucsb.edu.

[†] University of California, Santa Barbara.

[‡] San Diego State University.

- (1) Dertz, E. A.; Raymond, K. N. in *Iron Transport in Bacteria*; Payne, S., Crosa, J., Eds.; ASM Press: Washington, DC, 2004; pp 5–17; Winkelmann, G. *Biochem. Soc. Trans.* **2002**, *30*, 691–696.
- (2) Boukhalfa, H.; Crumbliss, A. L. *Biometals* **2002**, *15*, 325–339.
- (3) (a) Butler, A.; Martin, J. D. *Met. Ions Biol. Syst.* **2005**, *43*, 21–46. (b) Butler, A. *BioMetals* **2005**, *18*, 369–374. Kraemer, S. M.; Butler, A.; Borer, P., Cervini-Silva, J. *Rev. Mineral.: Mol. Geomicrobiol.* **2005**, *59*, 53–76.
- (4) Reid, R. T.; Live, D. H.; Faulkner, D. J.; Butler, A. *Nature* **1993**, *366*, 455–458. Holt, P. D.; Reid, R. R.; Lewis, B. L.; Luther, G. W., III; Butler, A. *Inorg. Chem.* **2005**, *44*, 7671–7677.
- (5) Martínez, J. S.; Zhang, G. P.; Holt, P. D.; Jung, H.-T.; Carrano, C. J.; Haygood, M. G.; Butler, A. *Science* **2000**, *287*, 1245–1247.
- (6) Haygood, M. G.; Holt, P. D.; Butler, A. *Limnol. Oceanogr.* **1993**, *38*, 1091–1097.
- (7) Hickford, S. J. H.; Küpper, F. F.; Zhang, G.; Carrano, C. J.; Blunt, J. W.; Butler, A. *J. Nat. Prod.* **2004**, *67*, 1897–1899.
- (8) Ito Y.; Butler, A. *Limnol. Oceanogr.* **2005**, *50*, 1918–1923.

(9) Gibson, F.; Magrath, D. I. *Biochim. Biophys. Acta* **1969**, *192*, 175–184.

(10) Neilands, J. B. *Can. J. Microbiol.* **1992**, *38*, 728–733

(11) Bull, C. T.; Carnegie, S. R.; Loper, J. E. *Phytopathology* **1996**, *86*, 260–266.

(12) Abrahamson, H. B.; Rezvani, A.B.; Brushmiller, J. G. *Inorg. Chim. Acta* **1994**, *226*, 117–127.

Fe(II) and release of CO₂. All the marine bacteria that produce the α -hydroxy carboxylic acid siderophores were isolated from the top 30 m of the open ocean, which is the mixed layer of the ocean. Thus, the ferric siderophore complexes are exposed to UV radiation from sunlight which promotes photooxidation of the siderophore and reduction of Fe(III). We have reported previously that photolysis of the Fe(III)–aquachelin siderophores under natural sunlight form a new ligand with a conditional stability constant for Fe(III) that is similar or slightly lower than the aquachelins themselves, concomitant with the reduction of Fe(III) to Fe(II).¹³ In addition the citrate-containing petrobactin¹⁴ and synechobactins⁸ are also photoreactive, producing Fe(II) and an oxidized ligand.

Given the fact that aerobactin is a siderophore produced by both marine and terrestrial bacteria, that it has been known for decades, and that it is a relatively simple symmetric structure, we have investigated the photoreactivity of the Fe(III)–aerobactin complex. During the course of our work, others have also begun to investigate the photoreactivity of ferric aerobactin.¹⁵ We report herein the structure elucidation of the photoproduct produced upon photolysis of Fe(III)–aerobactin and the affinity of the photoproduct for Fe(III). Interestingly, the aerobactin photoproduct complex facilitates uptake of Fe(III) by the source bacterium, *Vibrio sp.* DS40M5, similar to aerobactin-mediated Fe(III) uptake.

Experimental Methods

Isolation. Aerobactin was isolated from *Vibrio sp.* strain DS40M5 by modification of a previously reported procedure.⁶ Bacterial growth was carried out in artificial seawater medium (ASW) containing per liter, 15 g of NaCl, 0.75 g of KCl, 12 g of MgSO₄·7H₂O, 3 g of CaCl₂·2H₂O, 1 g of NH₄Cl, 2 g of casamino acids, and 0.1 g of glycerol phosphate (pH 7.8) for 7 days as 2-L cultures in 4-L flasks on a rotary shaker (110 rpm). After the bacterial cultures was pelleted by centrifugation, the decanted supernatant was acidified to pH 2.5 before addition of Amberlite XAD-2 resin to adsorb aerobactin, incubation for 24 h, and finally elution with 100% MeOH. The presence of siderophore in the methanol eluent was established either by the solution-phase chrome azurol S (CAS) assay containing the shuttle¹⁶ or by the color change following direct addition of methanolic FeCl₃.

Photolysis of Fe(III)–Aerobactin. Iron(III)–aerobactin was prepared by addition of FeCl₃·6H₂O in MeOH to apo-aerobactin at pH 8, and purified by HPLC (see below). Fe(III)–aerobactin (> 1 mM) was photolyzed with a 450-W mercury arc lamp for 5 h in Corex glass tubes.¹⁷ ESI-MS was used to verify the reaction was complete by monitoring the disappearance of Fe(III)–aerobactin at $m/z = 618$.

Purification of the Apo-photoproduct of Aerobactin. Photoproduct was deferrated by reaction of excess 8-hydroxyquinoline (HQ) in MeOH and extraction with chloroform to remove Fe(HQ)₃.

The remaining solution was concentrated by rotary evaporation. The apo-aerobactin photoproduct was purified by reversed-phase HPLC (preparative C4 column; VYDAC) running a gradient of 100% solvent A (with 0.01% trifluoroacetic acid) to 100% solvent B (60% methanol/0.01% trifluoroacetic acid) over 35 min. Under these conditions, the photoproduct typically eluted after ca. 25 min. HPLC fractions were screened for CAS activity, concentrated by evaporation (SpeedVac, Jouan model 10.10), checked for purity again by RP-HPLC using analytical columns, and freeze-dried.

Instrumental Methods. Electrospray-ionization mass spectrometry (ESI-MS) spectra were obtained on a Micromass QTOF-2 mass spectrometer using MassLynx software (Manchester, UK). Samples were run in doubly distilled H₂O or a MeOH/CH₃CN mixture with or without 0.01% TFA. For exact mass measurements, an internal standard of known mass and similar molecular weight (H9985, an octapeptide with $m/z = 829.5393$ of the protonated species, provided by Bachem California, Inc., Torrance, CA) was co-infused with the aerobactin photoproduct. MS/MS spectra utilized a collision voltage between 20 and 30 V and argon as the collision gas.

NMR experiments (i.e., ¹H, ¹³C, DEPT, and HMQC) were run at 25 °C in either *d*₆-DMSO or D₂O on a Varian INOVA 500 MHz NMR spectrometer using standard pulse sequences obtained from the VNMR software. UV–vis spectra were recorded on a Cary 300 spectrophotometer.

Circular dichroism (CD) spectra were recorded at pH 6.0 on a 500 μ M aqueous sample of Fe-photoproduct from 200 to 450 nm at 1 nm intervals (10 scans/nm, 1 s/scan) on a CD spectrometer 202 (AVIV Instruments, Lakewood, NJ).

Thermodynamic Measurements. Standard carbonate-free solutions of KOH were prepared from Baker “Dilut-It” ampules using boiled doubly deionized water (Nanopure) water and were stored under Ascarite-scrubbed argon. Base solutions were standardized with KHP to the phenolphthalein end point. The absence of carbonate (<2%) was confirmed by Grans plots. Iron solutions were prepared from Fe(NO₃)₃·9H₂O in 0.1 M HNO₃, and the exact iron concentration determined by EDTA titration with Variamine Blue as an indicator. Excess acid in the iron solution was determined by passing an aliquot through a well-washed sample of the acid form of AG 50W-X8 cation-exchange resin (Bio-Rad) and titrating the liberated acid. The excess acid was the difference between the total acid and 3 \times the known iron concentration.

Spectrophotometric and potentiometric titrations were performed in a jacketed three-necked titration vessel connected to a constant-temperature water bath and held at 25.0(1) °C. The hydrogen ion concentration was measured using a Radiometer PHM240 pH meter with a pHC4406 combination electrode, which was standardized with a three-buffer sequence and corrected (as needed) to read the negative log of the hydrogen ion concentration directly using dilute HNO₃ solutions. Titrant was added to the cell, which was kept under a blanket of Ascarite-scrubbed argon gas, with a Gilmont microburet.

The low pH obtained upon mixing iron(III) with a solution of the apo-photoproduct indicates that a considerable degree of chelate formation occurs prior to the addition of any base. Since no significant fraction of free metal is present, it is not possible to obtain the overall formation constant from titration data directly. Therefore, the EDTA competition method was used to obtain the desired formation constant.¹⁸ Solutions for these measurements were prepared by adding a known quantity of iron stock to a 50 mM

(13) Barbeau, K.; Rue, E. L.; Bruland, K. W.; Butler, A. *Nature* **2001**, *413*, 409–413.

(14) Barbeau, K.; Zhang, G.; Live, D. H.; Butler, A. *J. Am. Chem. Soc.* **2002**, *124*, 378–379. Bergeron, R. J.; Huang, G.; Smith, R. E.; Bharti, N.; McManis, J. S.; Butler, A., *Tetrahedron* **2003**, *59*, 2007–2014.

(15) Borer, P. M.; Sulzberger, B.; Reichard, P.; Kraemer, S. M. *Marine Chem.* **2005**, *93*, 179–193.

(16) Schwyn, B.; Neilands, J. B. *Anal. Biochem.* **1987**, *160*, 47–56.

(17) Stone, K. J.; Little, R. D. *J. Am. Chem. Soc.* **1996**, *118*, 2495–2505.

(18) Harris, W. R.; Carrano, J. C.; Raymond, K. N. *J. Am. Chem. Soc.* **1979**, *101*, 2722–2727.

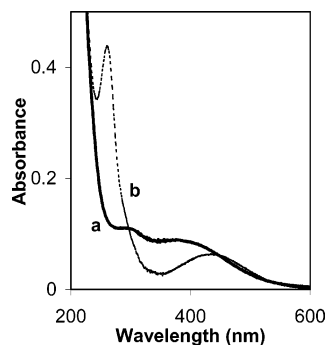


Figure 1. UV-vis spectra of (a, solid line) 54 μM Fe(III)-aerobactin at pH 8 (in UV-irradiated seawater) and (b, dashed line) after photolysis of solution in (a) in natural sunlight in a quartz flask for a period of ca. 8 h.

BICENE buffer at pH 6.0 containing 0.1 M KNO_3 , a constant amount of ligand and varying quantities of EDTA in excess, and allowing them to come to equilibrium. The attainment of equilibrium was monitored by optical spectroscopy and appeared to be relatively rapid, but samples were left for 1 week as a precaution. The concentration of iron siderophore complex was measured by optical spectroscopy.

^{55}Fe Uptake Experiments. Bacterial cultures in stationary phase were centrifuged and resuspended in ASW to an optical density at 600 nm between 0.6 and 0.7, corresponding to approximately 0.15–0.2 mg dry weight bacterial biomass per milliliter. Bacteria were kept at 4 $^\circ\text{C}$ until use and then shaken at 130 rpm at room temperature for 30 min prior to addition of ^{55}Fe (III)-aerobactin-photoproduct or ^{55}Fe (III)-aerobactin. ^{55}Fe (III)-aerobactin and ^{55}Fe (III)-photoproduct were prepared by addition of a 10:9 molar excess of apo-aerobactin over Fe(III) or apo-photoproduct over Fe(III), in which the iron was a 1:10 isotopic dilution of $^{55}\text{FeCl}_3$ (NEN Life Sciences, MA) with natural-abundance FeCl_3 under acidic conditions. The pH was then raised to 7.5 by dilution to 1 mM in 30 mM NH_4HCO_3 buffer, which served as the stock solution of ^{55}Fe (III) used in bacterial incubations. At the end of a given incubation, 1 mL of bacterial suspension with added ^{55}Fe (III)-complex was pipetted onto Isopore (Millipore) membrane filters (0.1 μm VCTP) followed by washing with two aliquots of 5 mL of LiCl (100 mM) as a chaotrophic agent. To determine the extent of nonspecific binding of the iron complexes to the filters, a blank control was carried out with 1 μM ^{55}Fe (III)-aerobactin and ^{55}Fe (III)-photoproduct in the absence of bacterial cells.

Results and Discussion

Structure Elucidation. When Fe(III)-aerobactin is photolyzed in sunlight or by UV irradiation (Hg lamp) in aerobic solution, the UV-vis spectrum changes, indicating a transformation of the aerobactin ligand (Figure 1). The λ_{max} of Fe(III)-aerobactin¹⁸ at 398 nm shifts to 440 nm in the Fe(III)-photoproduct, while the λ_{max} at 296 nm of Fe(III)-aerobactin,¹⁸ which is the α -hydroxycarboxylate-to-Fe(III) charge-transfer, disappears and is replaced by a new λ_{max} at 260 nm in the photoproduct.

The ESI-MS of the Fe(III)-photoproduct is 572 amu for the $(\text{M} + \text{H})^+$ ion, which is a loss of 46 amu from that of the parent Fe(III)-aerobactin $(\text{M} + 2\text{H})^+$ ion at 618 amu. This loss of 46 amu corresponds to loss of CO_2 plus two protons, similar to the results of photolysis of ferric petrobactin.^{14,7} Removal of iron(III) from the aerobactin photo-

Table 1. NMR Assignments for the Photoproduct of Aerobactin^a

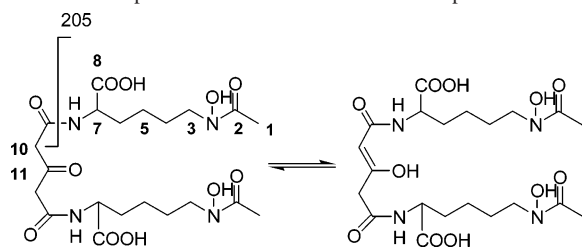
carbon number	^{13}C (δ)	^1H (δ)
3-ketoglutarate		
C11	199.3	
C10	46.7	3.4
C9	170.2	
N-H		8.3
lysine		
C8	173.4	
C7	51.9	4.1
C6	30.8	1.2–1.5
C5	22.4	1.2–1.5
C4	25.9	1.2–1.5
C3	50.1	3.4
N-acetyl		
N-OH		9.7
C2	165.8	
C1	20.3	1.9

^a 3 mg of aerobactin photoproduct dissolved in 1 mL of d_6 -DMSO.

product with excess HQ allowed for the isolation of the apo-photoproduct and its complete characterization by MS and NMR. The apo-photoproduct has an exact mass of 541.2148 amu, which gives a molecular formula for the $[\text{M} + \text{Na}]^+$ ion of $\text{C}_{21}\text{H}_{34}\text{N}_4\text{O}_{11}\text{Na}$. MS/MS on the parent ion produces two fragments at 315 and 205 amu. The latter represents the *N*-hydroxy-*N*-acetyl lysine fragment also seen in aerobactin fragmentation. MS/MS on the 315 amu daughter ion produces another 205 amu fragment (i.e., the other *N*-hydroxy-*N*-acetyl lysine arm), suggesting that the photolysis only affects the central citryl portion of the molecule while leaving the *N*-hydroxy-*N*-acetyl lysine moieties untouched.

The ^1H NMR spectrum of the photoproduct in D_2O is similar to that reported for aerobactin;⁹ however, the expected doublet of doublets signal at ca. 2.5 ppm characteristic of the citrate methylene protons is absent. The lack of any resonances attributable to the expected 3-ketoglutarate fragment was puzzling initially; however, keto-enol tautomeric equilibration would provide a pathway by which the methylene protons could exchange with deuterium in the solvent. In fact, the exchange of the methylene protons of the 3-ketoglutarate with D_2O was confirmed by ESI-MS, which showed an increase of 10 amu. Thus, in addition to the six readily exchangeable carboxylate, hydroxamate, and amide protons, four additional protons exchange with deuterium, corresponding to the four missing methylene protons in the ^1H spectrum of the 3-ketoglutarate moiety scrambled by the keto-enol interconversion.

Proton NMR of the photoproduct in d_6 -DMSO shows that only one species is present in solution and that the protons on the carboxylic acids, the hydroxamic acids, and the amides are now observable at ca. 12, 9.7, and 8.3 ppm, respectively. The ^{13}C NMR spectrum in the same solvent shows 11 sharp carbon resonances (Table 1) expected for the symmetrical keto form of the photoproduct. The DEPT spectrum shows that the resonance at 20.3 ppm is the acetyl methyl carbon, the resonance at 51.9 ppm is the C_α carbon of lysine, the resonances at 50.1, 46.7, 30.8, 25.9, and 22.4 ppm are methylene carbons, and the resonances at 199.3, 173.4, 170.2, and 165.8 are carbonyl carbons. The ^{13}C resonances at 46.7 and 199.3 ppm, i.e., the methylene carbons and the carbonyl

Scheme 1. Proposed Structure of Aerobactin Photoproduct^a

^a The numbers of the carbon atoms correspond to the ¹³C NMR assignment (Table 1). The *N*-hydroxy-*N*-acetyl lysine arm (*m/z* = 205) corresponds to a peptide-derived terminal γ fragment.

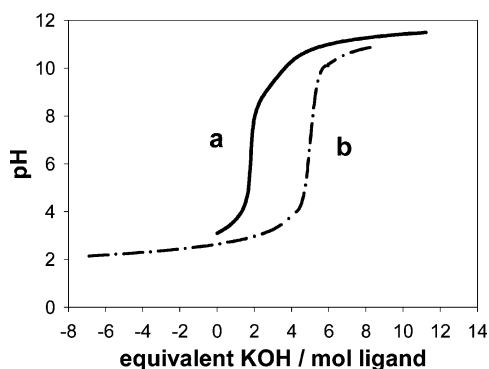


Figure 2. Potentiometric titration of (a) 0.87 mM apo-aerobactin photoproduct and (b) the Fe(III)–photoproduct complex after the addition of 0.85 mM Fe(III) to apo-aerobactin photoproduct in (a), as previously reported.¹⁸ Conditions: [KOH], 0.09972 M; *T*, 25.1 °C; *I*, 0.1 M KNO₃; initial volume, 10.0 mL.

carbon of 3-ketoglutarate, respectively, distinguish the photoproduct from aerobactin. The resonances attributable to the 3-ketoglutarate methylene protons, which were not distinct in the ¹H NMR spectrum obtained in DMSO, were identified by their correlation with the 46.7 ppm ¹³C resonance in an HMQC experiment also in DMSO. These protons apparently have accidental shift degeneracy with the 3.4 ppm resonances assigned to the methylene protons adjacent to the *N*-hydroxy-*N*-acetyl group. Integration confirms the presence of eight protons rather than four protons. Taken together, these data suggest that in DMSO the structure of the photoproduct is primarily in the keto form while in D₂O the evidence points to a keto–enol tautomeric interconversion (Scheme 1) leading to exchange of the methylene protons.

Ligand Protonation Equilibria. The potentiometric titration curve for the apo-aerobactin photoproduct is shown in Figure 2a. The data below pH 5 and the inflection at 2 equiv of base/mol of ligand represents the titration of the two free terminal carboxylic acid groups. Titration of both hydroxamic acid groups occurs above pH 8. Ligand protonation constants were determined from the nonlinear refinement of the data using the program PKAS developed by Motekaitis and Martell.¹⁹ The evaluated constants were 2.49-(3), 3.71(4), 8.64(1), and 9.62(1), which represent the terminal carboxylates and the two hydroxamate groups,

Table 2. Ligand Protonation Constants (log *K*) for Aerobactin¹⁹ and Photoproduct

	p <i>K</i> _a aerobactin ¹⁸	p <i>K</i> _a photoproduct
terminal COOH	3.11	2.49(3)
terminal COOH	3.48	3.71(4)
hydroxamic acid	8.93	8.64(1)
hydroxamic acid	9.44	9.62(1)
citryl COOH	4.31	
enol		10.80(3)
citryl OH	11 (estim.)	

respectively. At higher pH, an additional deprotonation was also indicated with a p*K*_a of 10.80(3). Attempts to fit the titration curve with a model containing only four dissociable protons resulted in a 10-fold worse standard deviation of fit. The measured constants are comparable to those of the parent siderophore aerobactin (Table 2). The highest p*K*_a in the photoproduct is in the range expected for the deprotonation of an enolate group in the β -diketone-like structure expected to be present on the basis of the MS and NMR data and is so assigned.

Metal Ligand Equilibria. Spectrophotometric titrations and ESI-MS demonstrate that the aerobactin photoproduct coordinates iron(III) with a 1:1 stoichiometry. The CD spectrum of Fe(III)–photoproduct has negative CD bands at 330 (–10.8) and 379 nm (–15.7) and a positive band at 475 nm (+ 4.5) similar to that reported previously for Fe(III)–aerobactin,¹⁸ indicating retention of the Λ chirality around the iron.

The potentiometric titration curve for an equimolar solution of aerobactin photoproduct and Fe(III) is shown in Figure 2b. Under experimentally accessible conditions, the lack of any free metal at equilibrium precluded refinement of the overall formation constant. Nevertheless, a number of important points can be ascertained from the rather featureless curve. Above pH 7, five protons are released upon iron(III) coordination, indicating that in addition to the four readily titratable protons on the ligand (i.e., two H⁺s released on complexation of the hydroxamates and two H⁺s for the pendant carboxylic acids), an additional proton, almost certainly from the β -diketoenolate, is also released upon iron(III) complexation. Spectrophotometric titrations could be used for quantitation of several of the pertinent metal–ligand equilibria. Starting at low pH, where the iron siderophore complex is completely soluble, and raising the pH from 2.0 to 2.9 brought about changes in the optical spectrum with a shift in λ_{max} from 467 to 440 nm and an increase in the absorbance. However, isosbestic behavior is not observed. Between pH 3.0 and 5.0, further changes in the optical spectrum corresponding to a shift in λ_{max} from 440 to 424 nm occur over which an isosbestic point is maintained (Figure 3a), despite the fact that three protons are removed over this range, as indicated by the titration curve. Thus, as with aerobactin,¹⁸ we interpret this behavior as indicating that two of the three deprotonations occur at the peripheral carboxylate groups which are not part of the metal coordination sphere and do not appreciably affect the optical spectrum. The system can therefore be treated via a nonlinear

(19) Motekaitis, R. F.; Martell, A. E. *Determination and Use of Stability Constants*, 2nd ed.; VCH Publishing: New York, 1992.

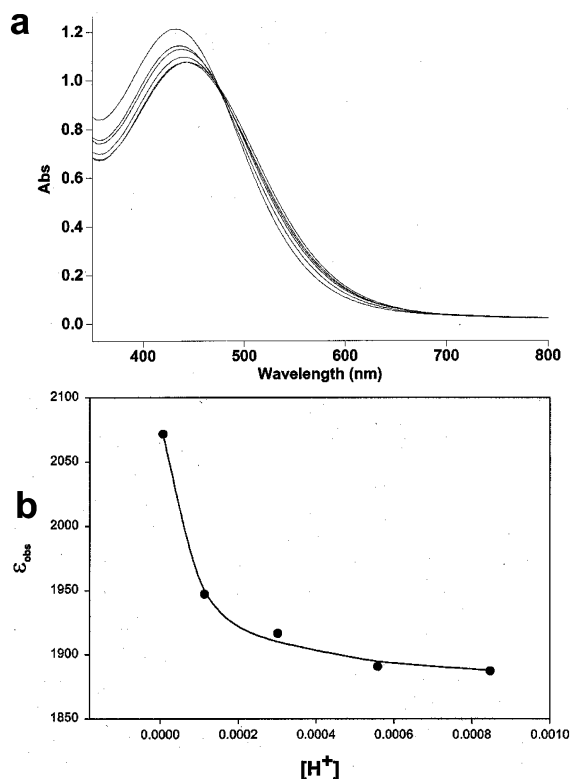


Figure 3. (a) Spectrophotometric titration of 0.59 mM Fe(III)-photoproduct from pH 2.93 to 5.16. (b) Nonlinear least-squares fit of the absorbance value at 435 nm to the Schwarzenbach equation. The $\log K_{\text{MHL}}$ is 4.22.

Schwarzenbach analysis (eq 1, Figure 3b)²⁰ as a single-proton equilibrium between FeL^- and FeHL as in eq 2 to give $\log K_{\text{MHL}}$ of 4.22(5), ϵ_{MHL} of 1873 $\text{M}^{-1} \text{cm}^{-1}$, and ϵ_{ML} of 2095 $\text{M}^{-1} \text{cm}^{-1}$.¹⁷

$$\epsilon_{\text{obsd}} = [1/K_{\text{MHL}}(\epsilon_{\text{ML}} - \epsilon_{\text{obsd}})/H^n] + \epsilon_{\text{MHL}} \quad (1)$$

where ϵ_{obsd} is the absorbance/[Fe], ϵ_{ML} is the extinction coefficient of the unprotonated complex, ϵ_{MHL} is the extinction coefficient of the protonated complex, K_{MHL} is the protonation constant, and H^n is the concentration of hydrogen ions where n is the number of protons involved.²⁰



EDTA Competition. Since direct measurement of the overall M-L binding constant was precluded, we utilized an indirect EDTA competition method to determine the ferric affinity constant. Using a 2–10-fold excess of EDTA over aerobactin photoproduct at pH 8.0, it is possible to set up a measurable competition of Fe(III) between the two ligands. The measured equilibrium constant, K_{m} , of 4.3(5) represents the reaction shown in eq 3:

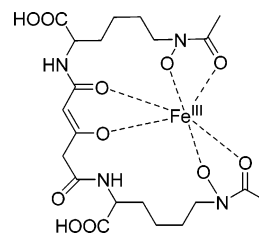


where photoproduct and EDTA represent the ligands in their all-protonated states. The conditional or pH-dependent

formation constant for the iron(III)-photoproduct is then given by eq 4.

$$K_{\text{Fepphoto}}^* = K_{\text{m}} K_{\text{FeEDTA}}^* \quad (4)$$

To obtain the standard pH-independent formation constant, which is written in terms of the fully deprotonated ligand states, it is necessary to correct the free siderophore and EDTA concentrations to that of their respective fully deprotonated forms using the appropriate α function. This calculation in turn requires knowledge of the protonation constants for the respective ligands. These values are known for Fe(III)-EDTA, as is the overall pH independent formation constant ($\log K_{\text{ML}} = 25.1$),²¹ and all of the five required constants have been measured for the photoproduct. Given these conditions, the overall formation constant, $\log K_{\text{ML}}$, for the Fe(III)-photoproduct complex is 28.6(5), a value that within experimental error is surprisingly similar to that of the parent iron(III)-aerobactin complex at 27.6(1). The proposed coordination for Fe(III) to the photoproduct is consistent with ligation by both hydroxamate groups and the β -ketoenolate, analogous to acetylacetonate coordination:



Iron Uptake into the Bacterium. The similar structure and stability constants of aerobactin and the aerobactin photoproduct for Fe(III) raises the question whether the photoproduct can mediate Fe(III) uptake into the bacterium. Initial experiments demonstrated that incubation of *Vibrio sp.* DS40M5 with 5 μM $^{55}\text{Fe(III)}$ -photoproduct for 10 min resulted in an uptake of $1.99 \pm 0.35 \mu\text{mol Fe/g}$ dry weight cell mass, whereas incubation of the bacteria with a mixture of $^{55}\text{Fe(III)}$ -photoproduct and 5 μM Fe(III)-aerobactin (i.e., natural abundance Fe(III), not ^{55}Fe) for 10 min resulted in $0.53 \pm 0.14 \mu\text{mol Fe/g}$ dry weight bacterial cell mass, suggesting that ^{55}Fe uptake mediated by photoproduct competes with Fe(III)-aerobactin-mediated iron uptake. Further investigations into the nature of the competition between photoproduct and aerobactin mediated iron uptake are in progress.

Conclusions

The photoreaction of Fe(III)-aerobactin results in the formation of a new ligand that has surprisingly similar features compared to the original siderophore. Structurally, the photoproduct differs only by the loss of the central carboxylic acid group, with an enol group (in mesomeric equilibrium in aqueous solution with the keto form) remaining on the former citrate backbone. Our results show that

(20) Schwarzenbach, G.; Schwarzenbach, K. *Helv. Chim. Acta* **1963**, *46*, 1390–1400.

(21) Martell, A. E.; Smith, R. M. *Critical Stability Constants*; Plenum Press: New York, 1974; Vol. 3, pp 161–166.

not only does the photoproduct result in a new ligand with similar physio-chemical properties but also one of similar physiological properties in that both forms facilitate iron acquisition by *Vibrio sp.* DS40M5 using the same, or a closely related, transport system. In addition, the extent to which phytoplanktonic communities can utilize siderophore-bound iron(III) and the photoproducts of siderophores complexed to iron(III) is of potential global significance.¹³

Acknowledgment. Funding from NIH Grant No. GM-38130 and The Center for Environmental BioInorganic Chemistry (CEBIC), an NSF Environmental Molecular

Science Institute (CHE-0221978) is gratefully acknowledged. We thank Margo Haygood (OHSU) for *Vibrio sp.* DS40M5 and for ongoing collaboration and Katherine Barbeau (SIO, UCSD) for helpful discussions. We thank James Pavlovich, Ph.D. (UCSB) for ESI-MS assistance and P. C. Ford (UCSB) and R. D. Little (UCSB) for photolysis equipment.

Supporting Information Available: HMQC of aerobactin photoproduct; ESI-MS of aerobactin and photoproduct. This material is available free of charge via the Internet at <http://pubs.acs.org>.

IC0604967